ORNL/TM-5419/V2

Calculations Pertaining to the Design of a Prebuncher for a 150-MeV Electron Linear Accelerator: II. Radial Motion

R. G. Alsmiller, Jr.
F. S. Alsmiller
J. Barish

OAK RIDGE NATIONAL LABORATORY
OPERATED BY UNION CARBIDE CORPORATION · FOR THE DEPARTMENT OF ENERGY

DISCLAIMER

Printed in the United States of America. Available from
National Technical Information Service
U.S. Department of Commerce
5285 Port Royal Road, Springfield, Virginia 22161
Price: Printed Copy $4.50; Microfiche $3.00

ORNL/TM-5419/V2

Contract No. W-7405-eng-26

Engineering Physics Division

Calculations Pertaining to the Design of a Prebuncher for a 150-MeV Electron Linear Accelerator: II. Radial Motion

R. G. Alsmiller, Jr.
F. S. Alsmiller†
J. Barish†

Date Published - May 1979

†Consultant
†Computer Sciences Division

OAK RIDGE NATIONAL LABORATORY
Oak Ridge, Tennessee 37830
operated by
UNION CARBIDE CORPORATION
for the
DEPARTMENT OF ENERGY

THIS PAGE

WAS INTENTIONALLY

LEFT BLANK

ACKNOWLEDGMENTS

Thanks are due to T. A. Lewis, R. W. Peelle and F. C. Maienschein of the Oak Ridge National Laboratory for many helpful discussions during the course of this work.

THIS PAGE

WAS INTENTIONALLY

LEFT BLANK

ABSTRACT

In a previous paper, calculated results based on a one-dimensional ballistic model were presented to indicate the extent to which a current pulse of 150-keV electrons containing 1 μC of charge and having a duration of 15 nsec (FWHM) could be bunched by a combination of accelerating and decelerating voltage gaps followed by a drift space. In the present paper a very approximate perturbation model is used to determine the extent to which the prebuncher performance determined previously is modified by radial electron motion. It is found that if a longitudinal magnetic field of 1 kG is applied in the region containing the voltage gaps and if a sufficiently strong longitudinal magnetic field ($\sim$ 3 kG) is applied in the drift space the prebuncher performance determined here is essentially the same as that shown in the previous paper.

1. INTRODUCTION

The Oak Ridge Electron Linear Accelerator (ORELA) was designed to produce intense short neutron pulses for measurements of neutron cross sections by time-of-flight techniques. It is proposed to improve ORELA for time-of-flight measurements by "prebunching" the electron beam before it enters the accelerator, that is, it is proposed to substantially reduce the initial pulse length without appreciably changing the charge in the pulse by passing the beam through a combination of voltage gaps and drift spaces before it enters the accelerator.

In a previous paper[1], hereinafter referred to as 1, calculated results based on an essentially one-dimensional model, were presented of the degree of bunching that can be achieved with various combinations of voltage gaps and drift spaces. Because of the large charge densities considered in 1, space charge effects were very large and were taken into account in the calculations. In 1 it was pointed out that in the vicinity of the voltage gaps the magnitude of the longitudinal magnetic field that can be produced experimentally to prevent radial spreading of the beam is very limited, but it was assumed that by applying a sufficiently large longitudinal magnetic field in the drift space following the gaps excessive radial spreading of the beam could be prevented. Here, calculated results similar to those given in 1, but with the radial motion of the electrons treated very approximately, are presented to test this assumption. The treatment of the radial motion is based on the assumption that the longitudinal motion of the electrons is unaffected by the radial motion. Since the "bunched" electron beam is useful only insofar as it will be accelerated by the existing accelerator, the results presented here, as in 1, include calculated

estimates of the fraction of the bunched electron beam that will be accelerated by ORELA.[2,3]

In Section 2 the calculational models are developed and discussed. In particular the major assumptions on which the calculations are based are enumerated in Section 2.2. In Section 3 the results are presented and discussed.

2. CALCULATIONAL PROCEDURE

2.1 Geometric Configuration and Physical Data

The cylindrically symmetric geometric configuration and the physical data considered here are the same as that considered in 1 in almost all details. The initial electron pulse shape, the voltage gap structure, and the time dependence of the voltages at both "accelerating" and "decelerating" gaps is the same as in 1. In particular, all of the results presented here are for the eight voltage gap configurations shown in Fig. 1 of 1. The gaps are assumed to be infinitesimally thin and voltage in each is turned on when the first electron reaches it. The variation of the externally imposed longitudinal component of the magnetic field with space is the same as that considered in 1 (see Fig. 1 of 1). In all cases considered here, the longitudinal magnetic field has a constant value of 1 kG for distances less than 275 cm after which it rises linearly and reaches its maximum value H_{zm} in 25 cm. Beyond 300 cm the longitudinal component of the magnetic field is constant at the value H_{zm}. This magnitude, H_{zm}, is varied to determine its effect on the prebuncher performance.

2.2 General Assumptions of the Model

The calculations in 1 and here are based on a variety of simplifying assumptions. To make these assumptions as explicit as possible they will be outlined before it is shown in the next section how they are implemented in the form of equations that are solved numerically. In 1 the beam entering the prebuncher was divided into "disks" with uniform radial density, fixed radius, and equal initial length in the z-direction, i.e., parallel to the magnetic field. The azimuthal motion of the electrons in each disk was based on the assumptions that the electrons are emitted from the cathode with zero initial azimuthal velocity and that the cathode is shielded from the magnetic field. This has the consequence that the electron orbits in the prebuncher encircle the axis of the conducting cylinder. The particular form of the magnetic field chosen resulted in azimuthal angular velocities that are proportional to the strength of the external longitudinal magnetic field divided by the total (relativistic) electron energy. The initial average velocity in the z-direction of all disks was taken to be the same, but the charge of the disks were varied to conform to the shape of the initial pulse (see Fig. 1 of 1). The average z-coordinate and velocity of each disk was calculated as a function of time from the relativisitc equations of motion. During the motion, disks interpenetrate, may be elongated or compressed in the z-direction, and may pass each other.

In the longitudinal disk motion considered here all of the above assumptions are retained except that of a constant radius of the disks. Here the radius of a disk (in the longitudinal equations) is allowed to take one of two constant values appropriated to the two different magnetic

field strengths used in the vicinity of the voltage gaps and in the drift space. This change was made because the radial motion considered here shows that the beam radius changes substantially with the strength of the magnetic field.

In the radial calculations presented here for the trajector of an individual electron the assumption is made that the longitudinal motion of the electron is essentially unaffected by the radial motion. The z-coordinates and velocities of all of the electrons in a given disk are constrained to be the same as the average values for that disk. Hence, except for the slight change noted in the last paragraph the longitudinal motion calculated here would be the same as that calculated in 1.

It is further assumed that the electron paths for the outer electrons in a given disk do not cross the paths of the inner electrons so that an electron that is initially on the periphery of a disk (now of variable radius) remains on the periphery throughout the motions.* As a consequence, only the radial motion of a representative peripheral electron in each disk must be determined to determine the spreading of the beam. This assumption is very drastic and, particularly in the presence of the z-wise bunching considered here, can be expected to give, at best, only very approximate results.

The space charge electric and magnetic fields on a particular disk, i, from the motion of any other disk, j, are computed with the assumption that

---

*A method of treating radial crossings and avoiding the assumption is given in Refs. 4 and 5. This method was not used here because in the present problem where 200 disks are required to obtain an adequate solution in the z-direction it would have necessitated very long computing times.

disk, j, has a radius that is time independent. As a consequence of this, the radial equation of disk, i, is independent of the radial equation for disk, j, and the computations are greatly simplied. It should be noted, however, that the radial equation for disk, i, is dependent on the longitudinal motion of disk, j, so the effects of the longitudinal bunching on the radial motion is taken into account.

2.3 Equations of Motion

Following 1, the equation of motion of an electron in the z-direction may be written as

$$\frac{1}{c}\frac{dp_z}{dt} = eE_z(z,r,t) + e\sum_{k=1}^{N_G} V_k(t)\delta(z_{Gk}-z) - e^2\left(\frac{r^2}{4m\gamma}\right) H_z(z)\frac{\partial H_z(z)}{\partial z} + e\,\beta_r\, H_\phi(z) \tag{1}$$

$$\gamma = \left\{1-\beta_z^2-\beta_r^2-\left[e\frac{rH_z(z)}{2m\gamma}\right]^2\right\}^{-1/2}$$

$$\beta_z = \frac{1}{c}\frac{dz}{dt} \tag{2}$$

$$\beta_r = \frac{1}{c}\frac{dr}{dt} \quad ,$$

where

z,r,ϕ = the polar coordinates of the electron,

c = the velocity of light,

p_z = the z component of the momentum of the electron multiplied by the velocity of light,

e = the electronic charge,

$E_z(z,r,t)$ = the longitudinal component of the space charge electric field,

N_G = the number of voltage gaps,

$V_k(t)$ = the time-dependent voltage on the kth voltage gap,

z_{Gk} = the position coordinate of the kth voltage gap,

$H_z(z)$ = the externally applied longitudinal magnetic field,

$H_\phi(z)$ = the azimuthal component of the magnetic field (due to the longitudinal motion of the electron in the prebuncher)

m = the rest energy of an electron.

In writing Eqs. (1) and (2) it has been assumed that only the externally applied radial and longitudinal magnetic fields are significant, i.e., the radial or longitudinal magnetic field due to the motion of the electrons in the prebuncher have been neglected. Also, it has been assumed that there is no externally applied azimuthal magnetic field. If there is assumed to be no radial motion so $\beta_r = 0$ then Eqs. (1) and (2) reduce to Eqs. (18) and (19) of 1. Here the assumption is made that β_r is small so that the terms involving β_r in Eqs. (1) and (2) may be neglected. This being the case one may proceed exactly as in 1, i.e., the "disk" approximation may be introduced, and obtain for the z-motion of the charge Q_i the equations

$$\frac{1}{c}\frac{dp_{zi}}{dt} = Q_i \sum_{\substack{j=1 \\ j\neq i}}^{N'} E_{sj}\,(z_i,z_j,\beta_j) + Q_i \sum_{k=1}^{N_G} V_k(t)\,\delta(z_{Gk}-z_i) - Q_i\, e \left[\frac{r_o^2(z_i)}{8m\gamma'_{zi}}\right] H_z(z_i)\,\frac{\partial H_z(z_i)}{\partial z_i} \qquad (i=1 \text{ to } N) \tag{3}$$

$$\Delta t_o = \frac{t_{oM}}{N} \tag{4}$$

$$\begin{aligned} N' &= \text{integer value of } \frac{t}{\Delta t_o} && t < t_{oM} \\ &= N && t \geq t_{oM} \end{aligned} \tag{5}$$

$$p_{zi} = M_i \gamma'_{zi} \beta_{zi} \tag{6}$$

$$\beta_{zi} = \frac{1}{c} \frac{d_{zi}}{dt} \tag{7}$$

$$\begin{aligned} \gamma'_{zi} &= \left[1-\beta_{zi}^2 - \left(\frac{er_o(z_i)H_z(z_i)}{2\sqrt{2}\, m\gamma'_{zi}} \right)^2 \right]^{-1/2} \\ &= \left[\frac{1 + \left(\frac{er_o(z_i)H_z(z_i)}{2\sqrt{2}\, m} \right)^2}{\left[1-\beta_{zi}^2 \right]} \right]^{1/2} \end{aligned} \tag{8}$$

where

p_{zi} = the z-component of the momentum of the charge Q_i, i.e., of the ith disk,

Q_i = the total charge of the ith disk,

$E_{sj}(z_i,z_j,\beta_j)$ = the longitudinal space charge electric field at

position z_i due to the charge Q_j,

$r_o(z)$ = the radius of the electron beam at position z (see discussion below)

t_{oM} = the total time required for the current pulse to enter the prebuncher (= 16.5 nsec),

N = the total number of disks considered,

M_i = the rest energy of the electrons in the charge Q_i.

Equations (3)-(8) differ from the longitudinal equations used in 1 only in that the radius of the electron beam, r_o, that was assumed to be constant in 1 has been indicated to be a function of z. In 1 the quantity r_o was assumed to be a constant even though the longitudinal magnetic field varied. Based on the radial motion considered here, it is found to be more consistent to assume that

$$r_o(z) = r_{oA} = \text{const.} \quad z \leq z_M + \frac{\Delta z_M}{2}$$
$$= r_{oB} = \text{const.} \quad z > z_M + \frac{\Delta z_M}{2} \quad , \tag{9}$$

where Δz_M = 25 cm and $z_M + \frac{\Delta z_M}{2}$ is the midpoint of the region where the longitudinal magnetic field changes its magnitude (see Fig. 1 of 1). The manner of calculating the constants r_{oA} and r_{oB} from the radial motion is explained later in this section. Of course the radius of the electron beam varies continuously with z so Eq. (9) is very approximate, but it is a better representation of the beam radius than was used in 1.

The longitudinal space charge field in Eq. (3) is given approximately by (see 1)

$$E_{sj}(z_i,z_j,\beta_j) = \frac{2}{r_o(z_i)r_o(z_j)} \sum_{r=1}^{\infty} \exp(-\gamma_{zj}\frac{\gamma_r}{a}|z_i-z_j|) \cdot \frac{2J_1\left(\gamma_r \frac{r_o(z_i)}{a}\right) J_1\left(\gamma_r \frac{r_o(z_j)}{a}\right)}{[\gamma_r J_1(\gamma_r)]^2} \text{sign}(z_i-z_j) \tag{10}$$

$$\gamma_{zi} = \left[1 - \beta_{zi}^2\right]^{1/2} \tag{11}$$

$$\gamma_r = \mu_r a$$
$$J_o(\mu_r a) = 0 \quad . \tag{12}$$

where

J_α = a Bessel function of the first kind.[6]

However, the presence of $r_o(z_i)$ and $r_o(z_j)$ in Eq. (10) greatly complicates the calculations and therefore the approximation of replacing $r_o(z_j)$ by $r_o(z_i)$ has been made to obtain

$$E_{sj}(z_i,z_j,\beta_j) = \frac{2}{r_o^2(z_i)} \sum_{r=1}^{\infty} \exp(-\gamma_{zj}\frac{\gamma_r}{a}|z_i-z_j|) \cdot \left[\frac{2J_1\left(\gamma_r \frac{r_o(z_i)}{a}\right)}{\gamma_r J_1(\gamma_r)}\right] \text{sign}(z_i-z_j) \quad , \tag{13}$$

Equation (13) differs from Eq. (10) only in the vicinity of $z_i = z_M + \frac{\Delta z_M}{2}$ where the longitudinal magnetic field is changing and in this region Eq. (10) is very approximate in any case.

The radial equation of motion of an electron may be written as

$$\frac{1}{c}\frac{dp_r}{dt} = eE_r(z,r,t) - e\beta_z H_\phi(z) + \frac{e}{c} r \frac{d\phi}{dt} H_z(z) + p_\phi \frac{d\phi}{dt} \tag{14}$$

$$p_r = m\gamma\beta_r$$

$$p_\phi = m\gamma \frac{r}{c}\frac{d\phi}{dt} \quad , \tag{15}$$

and using

$$\frac{1}{c}\frac{d\phi}{dt} = - e \frac{H_z(z)}{2m\gamma} \quad , \tag{16}$$

i.e., Eq. (17) from 1,

$$\frac{1}{c}\frac{dp_r}{dt} = eE_r(z,r,t) - e\beta_z H_\phi(z) - e^2 \frac{r}{m\gamma}\frac{H_z^2(z)}{4} \quad , \tag{17}$$

where

p_r = the r-component of the momentum of the electron,

$E_r(z,r,t)$ = the radial component of the space charge electric field,

and all of the other symbols have previously been defined. If now Eq. (17) is applied to a peripheral electron in disk i and if the disk approximation is used (see 1) for the radial electric and azimuthal magnetic fields one obtains

$$\begin{aligned}\frac{1}{c}\frac{dp_{ri}}{dt} = e \sum_{j=1}^{N'} & E_{rj}(z_i,r_i,z_j,r_j,\beta_j) \\ & - e\beta_{zi} \sum_{j=1}^{N'} H_{\phi j}(z_i,r_i,z_j,r_j,\beta_j) \\ & - e^2 \frac{r_i}{m\gamma_i}\frac{H_z^2(z_i)}{4} \qquad (i = 1 \text{ to } N)\end{aligned} \tag{18}$$

$$p_{ri} = m\gamma_i\beta_{ri} \tag{19}$$

$$\gamma_i = \left[1-\beta_{zi}^2-\beta_{ri}^2-\left(\frac{er_iH_z(z_i)}{2m\gamma_i}\right)^2\right]^{-1/2}, \tag{20}$$

where

r_i = the radius of disk i (now a function of time),

p_{ri} = the radial component of the momentum of an electron at r_i,

$E_{rj}, H_{\phi j}$ = the radial electric and azimuthal magnetic fields at the position z_i, r_i due to the charge Q_j.

Equations (18)-(20) are still the radial equations for a single electron. A basic assumption of the model used here is that the time dependence of the radius, r_i, of disk i may be identified with the time dependence of the radius of a peripheral electron in disk i. That is, it is assumed that the radial motion is sufficiently small that an electron that enters the pre-buncher on the periphery of a disk remains on the periphery of the disk throughout the motion. This also means that all of the charge Q_i at all times is assumed to lie inside the radius r_i.[7]

The set of equations represented by Eqs. (18)-(20) are still very complicated because the radial electric and azimuthal fields depend on both the z-coordinate and radial coordinate of all disks. In obtaining Eq. (3) the assumption was made that the radius of the disks had the value $r_o(z)$ (see Eq. (9)) so this same assumption - except for i = j - is also made in E_{rj} and $H_{\phi j}$ in Eq. (18). In 1 and in Eq. (3) the longitudinal electric

field of a charge Q_i on itself was assumed to be zero. In Eq. (18) the radial electric field and the azimuthal magnetic field from the charge Q_i are retained (i.e., $r_j = r_i$ in E_{rj} and $H_{\phi j}$) since the charge at small r in the ith disk exerts a force on the charge that is on the peripheral of the ith disk.

With these assumptions and with the expressions for the fields E_{rj} and $H_{\phi j}$ derived in the appendix the radial equation of motion becomes

$$\frac{1}{c}\frac{dp_{ri}}{dt} = eQ_i(1-\beta_{zi}^2)\gamma_{zi}\left\{\frac{4}{r_i a}\sum_{r=1}^{\infty}\frac{\left[J_1\left(\gamma_r\frac{r_i}{a}\right)\right]^2}{\gamma_r\left[J_1(\gamma_r)\right]^2}\right\}$$

$$+ eQ_j\sum_{\substack{j=1\\ j\neq i}}^{N'}(1-\beta_{zi}\beta_{zj})\gamma_{zj}$$

$$\cdot\left\{\frac{4}{r_o(z_i)a}\sum_{r=1}^{\infty} e^{-\gamma_{zj}\frac{\gamma_r}{a}|z_i-z_j|}\cdot\frac{J_1\left(\gamma_r\frac{r_o(z_i)}{a}\right)J_1\left(\gamma_r\frac{r_i}{a}\right)}{\gamma_r[J_1(\gamma_r)]^2}\right\} \qquad (21)$$

$$- e^2\frac{r_i}{m\gamma_i}\frac{H_z^2(z_i)}{4} \qquad (i = 1 \text{ to } N),$$

where all of the symbols have previously been defined, and it is to be noted that $r_o(z_j)$ has been approximated as in Eq. (13) by $r_o(z_i)$.

With the $r_j(t)$ determined for all of the disks it is possible to determine the average radius of the electron beam over various z regions and to identify these averages with the beam radius used in the calculation of the longitudinal motion. In determining these averages it seems most

appropriate to neglect those disks that correspond to the initial and final 1.5 nsec of the current pulse (see Fig. 1 of 1) since these disks, because they have smaller total charge than the majority of the disks, behave atypically. This amounts to neglecting end effects and will be done here. If r_{oA} and r_{oB} are the quantities used in Eq. (9) they are to be determined from the equations

$$r_{oA} = \sum_{(j)} \left[\frac{1}{t_j\left(z_M + \frac{\Delta z_M}{2}\right) - t_{jo}} \right] \cdot \int_{t_{jo}}^{t_j\left(z_M + \frac{\Delta z_M}{2}\right)} r_j(t)dt \tag{22}$$

$$r_{oB} = \sum_{(j)} \left[\frac{1}{t_j(z_{max}) - t_j\left(z_M + \frac{\Delta z_M}{2}\right)} \right] \cdot \int_{t_j\left(z_M + \frac{\Delta z_M}{2}\right)}^{t_j(z_{max})} r(t)dt \quad , \tag{23}$$

where

$\sum_{(j)}$ = sum over all disks except those that correspond to the initial and final 1.5 nsec of the initial current pulse (see discussion above and Fig. 1 of 1),

t_{oj} = the time when disk j enters the prebuncher at z = 0,

$t_j(z)$ = the time when the disk that enters the prebuncher at time t_{oj} is at position z,

z_{max} = the maximum length of the prebuncher (= 400 cm).

It should be noted that the $r_j(t)$ on the right of Eqs. (22) and (23) depend on r_{oA} and r_{oB} so Eqs. (22) and (23) are very implicit equations and, in fact, to satisfy them an iteration is required. It should also be noted that in the approximation used here the radial motion of the ith disk does not depend on the radial motion of the other disks.

2.4 Current Calculations and Fraction of the Current Pulse That Will Be Accelerated

To carry out the current calculations it is necessary to utilize the assumption that the charge density of a disk j is at all times uniformly distributed over the radial interval 0 to r_j. With this assumption, the current as a function of time at a fixed z is calculated in much the same manner as in 1. The only difference being that it is assumed that the entrance hole into the accelerator has a radius r_o' so that for a disk j all of the charge that is outside of the radius r_o' does not enter the accelerator. With this assumption, Eq. (35) of 1 becomes

$$I_j(z,t) = F(t,t_j,t_{j+1}) \cdot \frac{1}{2}\left[Q_j F_r(t_j)+Q_{j+1}F_r(t_{j+1})\right] \tag{24}$$

$$F(t,t_j,t_{j+1}) = [\theta(t_{j+1}-t)\theta(t-t_j)\theta(t_{j+1}-t_j) + \theta(t_j-t)\theta(t-t_{j+1})\theta(t_j-t_{j+1})] \tag{25}$$

$$\theta(x) = 1 \qquad x > 0$$
$$= 0 \qquad x < 0 \tag{26}$$

$$F_r(t_j) = \left(\frac{r_o'}{r_j(t_j)}\right)^2 \qquad r_j(t_j) > r_o'$$
$$= 1 \qquad r_j(t_j) \leq r_o' \ , \tag{27}$$

where

$I_j(z,t)$ = the current at z at time t that has a radius < r_o' due to the current that enters the prebuncher in the time interval t_{oj} and $t_{o,j+1}$,

t_j = the time when the center of charge Q_j that enters the prebuncher at time t_{oj} is at the position z,

r_o' = the radius of the hole into the accelerator.

Equation (24) differs from Eq. (35) of 1 in that the factor $F_r(t_j)$ and $F_r(t_{j+1})$ have been introduced. In 1 the radius of all disks were assumed to be r_o and r_o' was taken to be equal to r_o so that these factors were always unity. Here $r_j(t_j)$ may be larger than unity so these factors may be less than unity corresponding to the fact that charge may be lost at the entrance to the accelerator if the radius of a disk is larger than the hole into the accelerator. All of the discussions in 1 concerning the situation when a disk does not reach the depth z apply here as in 1. The total current, I(z,t) that enters the accelerator at position z at time t may be written

$$I(z,t) = \sum_{j=1}^{N'-1} I_j(z,t) \quad . \tag{28}$$

Only a fraction of the current pulse that is incident on the accelerator will actually be accelerated and emerge from the accelerator and it is desirable to obtain estimates of this fraction. With the current defined by Eq.(28) upper and lower limits on the current that will be accelerated may be calculated in the same manner as in 1, i.e., Eqs. (53) and (58) of 1 may be applied, and this was done to obtain the results presented here. As explained in 1 the upper and lower limits

on the current that will be accelerated are obtained because of the approximation that are made in the beam loading theory that is used.

3. RESULTS AND DISCUSSION

In this section calculated results for two cases of interest are presented and discussed. All of the results presented here are for the eight voltage gap configurations considered in 1. In all cases, the radius of the conducting cylinder, a, is 2.5 cm and the radius of the hole into the accelerator, r_o', is 0.4 cm. The total charge in the incident beam is 1 μC.

To carry out the calculations it is also necessary to specify the value of β_r for each disk at the entrance to the prebuncher. In obtaining the results in Figs. 1 and 2 it has been assumed that $\frac{\beta_r}{\beta_z} = .04$ for all disks at the entrance to the prebuncher.* This is, however, relatively unimportant because the results are quite insensitive to this value.

In all cases the longitudinal magnetic field has a constant value of 1 kG for distances of less than 275 cm after which it rises linearly and reaches its maximum value, H_{zm}, in 25 cm. Beyond 300 cm the longitudinal component of the magnetic field is constant at the value H_{zm}. In obtaining the results presented here, values of H_{zm} of 2 kG and 3 kG have been considered.

Before discussing the current that will be accelerated as a function of time it is necessary to consider the values of r_{oA} and r_{oB} (see Eq. (13)) that were used in the longitudinal calculations and the values of

*This value was obtained from an analysis of the ORELA electron gun by J.R.M. Vaughan of the Electron Tube Division of the Litton Corporation.

r_{oA} and r_{oB} (see Eqs. (22) and (23)) that were obtained from the averaged radial calculations. For the two cases considered here these values are shown in Table 1. The values used in the longitudinal calculations are very nearly the same as those obtained from the radial calculations and thus in this very limited sense the two calculations are consistent.

Table 1

Values of the Average Beam Radii Used in the Longitudinal Calculations and Determined from the Radial Calculations

	Longitudinal Calculation*		Radial Calculation+	
H_{zm}	r_{oA}	r_{oB}	r_{oA}	r_{oB}
kG	(cm)	(cm)	(cm)	(cm)
2	0.36	0.25	0.37	0.26
3	0.36	0.19	0.37	0.20

*See Eq. (9)

+See Eqs. (22) and (23)

In Figs. 1 and 2 the calculated results for the case H_{zm} equal 2 kG and 3 kG, respectively, are given. The results presented in each figure represent the current as a function of time (at the entrance to the accelerator) that will be accelerated for specific values of the length, L, of the prebuncher. In each figure the results shown by plotted points are for the case of no radial motion and the histograms give the results when radial motion is included. The plotted points, of course, also represent histograms. For each L value considered, the zero of time is taken to be the time when the first electron enters the accelerator. For each L value considered the current as a function of time is given "without beam loading" and "with beam loading." As explained in 1, the values

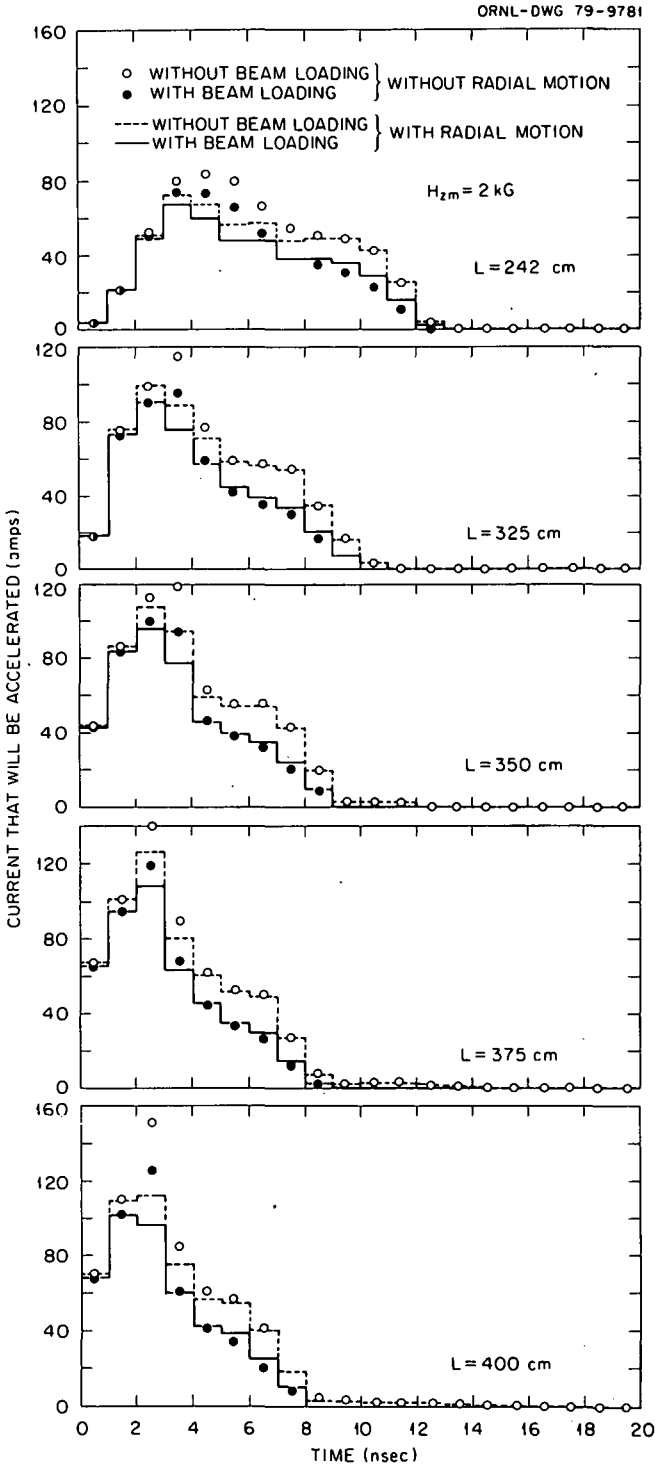

Fig. 1. Current that will be accelerated vs time.

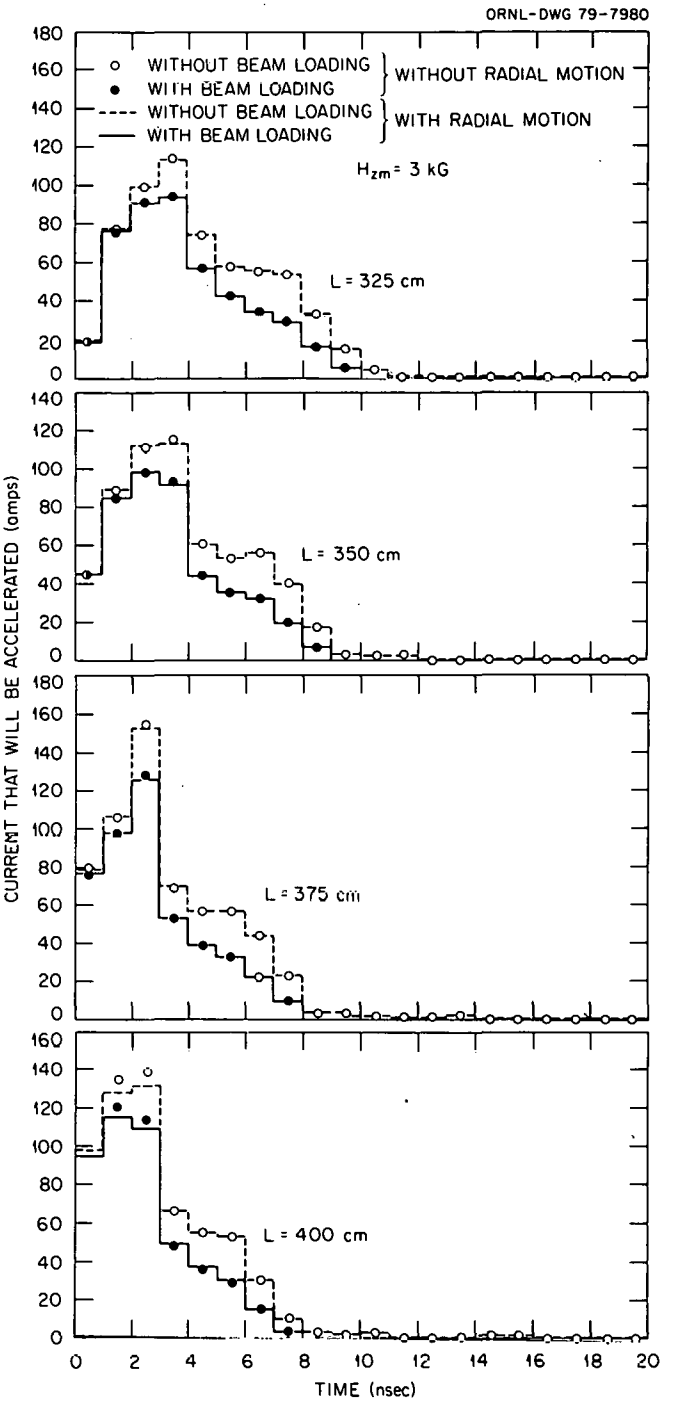

Fig. 2. Current that will be accelerated vs time.

"without beam loading" are an upper limit of the current that will be accelerated and the values "with beam loading" are a lower limit on the current that will be accelerated. In Table 2 the values of the total charge that will be accelerated and the standard deviation of the time distribution of the current that will be accelerated are given for each of the histograms in both Figs. 1 and 2. The values given in Table 2 are determined from the equations

$$Q_{\alpha\beta}(L) = \int_0^\infty I_{\alpha\beta}(L,t)dt \tag{29}$$

$$\bar{t}_{\alpha\beta}(L) = \frac{1}{Q_{\alpha\beta}(L)} \int_0^\infty I_{\alpha\beta}(L,t)tdt \tag{30}$$

$$\sigma_{\alpha\beta}(L) = \left[\frac{1}{Q_{\alpha\beta}(L)} \int_0^\infty I_{\alpha\beta}(L,t)[t-\bar{t}_{\alpha\beta}(L)]^2 dt\right]^{1/2} , \tag{31}$$

where

$I_{\alpha\beta}(L,t)$ = the current that will be accelerated as a function of time if the prebuncher has length L,

Table 2

Total Charge That Will be Accelerated and the Standard Deviation of the Accelerated Current Distribution (Results are given for each of the histograms in Figs. 1 and 2)

L (cm)	Q_{Uz} (μC)	Q_{Lz} (μC)	Q_{Ur} (μC)	Q_{Lr} (μC)	σ_{Uz} (nsec)	σ_{Lz} (nsec)	σ_{Ur} (nsec)	σ_{Lr} (nsec)
				H_{zm} = 2 kG				
242	0.62	0.48	0.55	0.45	3.1	2.6	3.1	2.9
325	0.61	0.46	0.59	0.46	2.5	2.1	2.7	2.3
350	0.61	0.46	0.57	0.45	2.4	2.0	2.5	2.1
375	0.61	0.46	0.57	0.45	2.4	1.9	2.5	1.9
400	0.61	0.46	0.55	0.44	2.3	1.8	2.3	1.9
				H_{zm} = 3 kG				
325	0.61	0.46	0.61	0.46	2.5	2.1	2.5	2.1
350	0.61	0.46	0.61	0.46	2.4	2.0	2.4	2.0
375	0.61	0.46	0.60	0.46	2.4	1.8	2.3	1.8
400	0.61	0.46	0.59	0.45	2.3	1.7	2.3	1.7

and α takes values U (meaning upper) for the case of no beam loading and L (meaning lower) for the case with beam loading and β takes values z for the case of no radial motion and r (meaning radial) for the case with radial motion.

The data at the top of Fig. 1 (H_{zm} = 2 kG) for L = 242 cm corresponds to the case when there is no drift space, i.e., when the electron beam enters the accelerator immediately after passing through the last voltage gap. The other L values considered in Fig. 1 correspond to increasingly longer drift spaces. For all of the L values considered in Fig. 1, the

open circles differ noticeably from the dashed histograms and the closed circles differ noticeably from the solid histograms. This indicates that there is some degradation of the prebuncher performance, i.e., of the bunching and of the charge that will be accelerated, due to radial motion when H_{zm} = 2 kG. The amount of degradation is, however, small, and is hardly noticeable from the integral values given in Table 2. It should be noted that for all of the L values considered in Fig. 1, there is a "tail" on the current distribution calculated without beam loading (open circles and dashed histograms). This "tail" corresponds to particles that lag behind the main pulse and were shown in some cases in 1. In Fig. 1 the tails are shown only out to 20 nsec, but they do extend beyond this time. It is important to note that the tails occur only when there is no beam loading, i.e., on the upper bounds. Since the "tails" occur only on the upper bounds as calculated here and not on the lower bounds the actual extent to which these tails will occur experimentally is not known from the present calculations.

Before leaving Fig. 1 it is interesting to note that at the larger times the solid dots are often below the solid histogram, i.e., at the later times and when beam loading is considered more charge is accelerated when radial motion is considered than is accelerated when radial motion is neglected. This is due to the fact that in the approximation used here the magnitude of beam loading is dependent on the total amount of charge that has entered the accelerator before a given electron enters the accelerator, and since in the presence of radial motion less charge enters the accelerator at early time the effects of beam loading are reduced on those electrons that enter the accelerator at the later times.

In Fig. 2 results similar to those given in Fig. 1 are presented for the case of H_{zm} = 3 kG. Data for L = 242 cm are not given in Fig. 2 because it would be the same as that shown in Fig. 1. In Fig. 2 the difference between the plotted points and the histogram values are, for practical purposes, negligible at all L values. This is also apparent from the values in Table 2. Thus, based on the very approximate model considered here the performance of the prebuncher will not be substantially affected by radial motion provided that a sufficiently strong longitudinal magnetic field ($\sim$ 3 kG) is applied over the region of the drift space.

THIS PAGE

WAS INTENTIONALLY

LEFT BLANK

Appendix 1

RADIAL ELECTRIC AND AZIMUTHAL MAGNETIC FIELDS

In this appendix the expressions used for the radial electric and azimuthal magnetic fields from a charge Q_j are derived. In the derivation only the longitudinal motion of the charge Q_j is considered and the acceleration of the charge Q_j is neglected so the fields must be considered to be very approximate.

The potential of a point charge at rest inside a conducting cylinder (assumed infinite in length) may be written[6]

$$V' = \frac{2e}{a^2} \sum_{r=1}^{\infty} \sum_{s=0}^{\infty} (2-\delta_s^0) \cdot e^{-[\mu_r|z_i'-z_j'|]} \cdot \frac{J_s(\mu_r b') J_s(\mu_r \rho')}{\mu_r [J_{s+1}(\mu_r a)]^2} \cdot \cos s(\phi'-\phi_0') \quad , \tag{A1.1}$$

where

a = the radius of the conducting cylinder,

z_j', b', ϕ_0' = the polar coordinates of a point charge in its rest system,

z', ρ', ϕ' = the polar coordinates of the field point in the rest system of the point charge,

J_s = a Bessel function of the first kind[6],

$$\delta_s^0 = 1 \text{ if } s = 0$$
$$= 0 \text{ if } s \neq 0, \tag{A1.2}$$

and μ_r is defined from the zeros of J_0 by the equation

$$J_0(\mu_r a) = 0. \tag{A1.3}$$

The electric field in the radial direction may be written

$$E'_{\rho'} = -\frac{\partial V'}{\partial \rho'} \quad , \tag{A1.4}$$

so

$$E'_{\rho'} = -\frac{2e}{a^2} \sum_{r=1}^{\infty} \sum_{s=0}^{\infty} (2-\delta_s{}^0)\, e^{-[\mu_r |z'_i - z'_j|]} \cdot \frac{J_s(\mu_r b')\frac{\partial}{\partial \rho'} J_s(\mu_r \rho')}{\mu_r [J_{s+1}(\mu_r a)]^2} \cos s(\phi' - \phi_0) \quad . \tag{A1.5}$$

Equation (A1.5) is the radial electric field in the system where the point charge is at rest. If the point charge is moving in the z-direction with a velocity $c\beta_{zj}$ and if it is assumed that the Lorentz transformation is valid when the conducting cylinder is present one has [8]

$$E_\rho = \gamma_{zj} E'_{\rho'} \tag{A1.6}$$

$$H_\phi = \gamma_{zj} \beta_{zj} E'_{\rho'} \tag{A1.7}$$

$$\gamma_{zj} = (1-\beta_{zj}^2)^{-1/2} \tag{A1.8}$$

$$z'_i - z'_j = \gamma_{zj}(z_i - z_j) \tag{A1.9}$$

$$\rho = \rho' \tag{A1.10}$$

$$\phi = \phi' \tag{A1.11}$$

$$b = b' \tag{A1.12}$$

$$\phi_o = \phi_o' \tag{A1.13}$$

so

$$E_\rho - \beta_{zi} H_\phi = (1-\beta_{zi}\beta_{zj})\gamma_{zj} E'_{\rho'} \quad . \tag{A1.14}$$

It is to be noted that in Eq. (A1.6) to (A1.14) only the longitudinal motion of the point charge has been considered and its acceleration has been neglected.

Equation (A1.14) gives the fields from a point charge, but to obtain the fields used in the body of the paper it is necessary to integrate over the charge density of the source disk. That is

$$\underline{E}_{\rho j} - \beta_{zi} H_{\phi j} = -\frac{1}{e} \int_{\Delta z_j} dz_j \int_0^{2\pi} d\phi_\phi \int_0^{r_j} bdb \cdot q_j (1-\beta_{zi}\beta_{zj})\gamma_{zj} E'_{\rho'} \tag{A1.15}$$

$$Q_j = \int_{\Delta z_j} dz_j \int_0^{2\pi} d\phi_o \int_0^{r_j} bdb \quad q_j \ , \tag{A1.16}$$

where

$E_{\rho j}$ = the radial electric field at z and ρ due to disk j,

$H_{\phi j}$ = the azimuthal magnetic field at z and ρ due to disk j,

q_j = the charge density of disk j,

Δz_j = the longitudinal extent of disk j,

r_j = the radius of disk j,

Q_j = the total charge of disk j .

Assuming that the charge density is constant and carrying out the integral over dz_j, using the mean value theorem,

$$
\begin{aligned}
E_{\rho j} - \beta_{zi} H_{\phi j} &= - q_j \Delta z_j (1-\beta_{zi}\beta_{zj})\gamma_{zj} \\
&\cdot \int_0^{2\pi} d\phi_o \int_0^{r_j} b\,db \\
&\cdot \frac{2}{a^2} \sum_{r=1}^{\infty} \sum_{s=0}^{\infty} (2-\delta_s{}^0) \\
&\cdot e^{-\mu_r \gamma_{zj} |z_i - z_j|} \\
&\cdot \frac{J_s(\mu_r b)\frac{\partial}{\partial \rho} J_s(\mu_r \rho)}{\mu_r [J_{s+1}(\mu_r a)]} \cos s(\phi-\phi_o)
\end{aligned}
\qquad \text{(A1.17)}
$$

where now z_j is the z-coordinate of disk j and β_{zj} is the z-velocity of this disk. The integrals and derivatives in (A1.17) may be carried out in a straightforward manner (see Appendix A of Ref. 1) to give

$$E_{\rho j} - \beta_{zi} H_{\phi j} = Q_j (1-\beta_{zi}\beta_{zj}) \gamma_{zj} \cdot \frac{4}{a r_j} \sum_{r=1}^{\infty} e^{-\gamma_{zj} u_r |z-z_j|} \cdot \frac{J_1(u_r r_j) J_1(u_r \rho)}{\gamma_r [J_1(\gamma_r)]^2} \qquad \text{(A1.18)}$$

where

$$\gamma_r = \mu_r a \quad . \qquad \text{(A1.19)}$$

In the approximation used here Eq. (A1.18) is valid for an arbitrary ρ so it is valid for $\rho = r_i$ as it is used in the body of the paper. Furthermore, Eq. (A1.18) is valid for any r_j so it is valid for $r_j = r_o(z_j)$. In the body of the paper the approximation is used that $r_j = r_o(z_i)$; that is, the same approximation is made here as was made in Eq. (13). Here, as in Eq. (13), this modifies the fields only in the region where the longitudinal magnetic field is changing appreciably and greatly simplifies the computations. Equation (A1.18) in any case must, of course, be considered to be very approximate because of the many assumptions that were used in the derivation.

REFERENCES

1. R. G. Alsmiller, Jr. et al., "Calculations Pertaining to the Design of a Prebuncher for an Electron Linear Accelerator," ORNL/TM-5419 (1977) (to be published with appendices omitted in Particle Accelerators).
2. N. C. Pering and T. A. Lewis, "Performance of 140 MeV High Current Short Pulse Linear at ORNL: IEEE Trans. on Nucl. Sci., NS-16(3) 316 (1969).
3. T. A. Lewis, "ORELA Performance," ORNL/TM-5112, Oak Ridge National Laboratory (1976).
4. J. E. Rowe, Nonlinear Electron-Wave Interaction Phenomena, Academic Press, New York, 1965.
5. P. J. Tallerico, "Transverse Effects in the High-Power Multicavity Klystron," Los Alamos MP Division Internal Report, MP-2-9 (1970). Private communiction from P. J. Tallerico of Los Alamos Scientific Laboratory, Los Alamos, New Mexico.
6. W. R. Smythe, Static and Dynamic Electricity, McGraw-Hill Book Co., Inc., New York, NY (Third Edition) 1968.
7. G. R. Brewer, "Focusing of High Density Electron Beams," in Focusing of Charged Particles, Ed. by A. Septier Academic Press, New York, 1967.
8. J. A. Stratton, Electromagnetic Theory, McGraw Hill, New York, 1941.

ORNL/TM-5419/V2

Internal Distribution

1. L. S. Abbott
2-6. F. S. Alsmiller
7-26. R. G. Alsmiller, Jr.
27-31. J. Barish
32. A. A. Brooks
33. H. A. Carter
34. J. W. T. Dabbs
35. G. DeSaussure
36. T. A. Gabriel
37. H. Goldstein (Consultant)
38. J. A. Harvey
39. T. A. Lewis
40. R. A. Lillie
41. J. L. Lucius
42. F. C. Maienschein
43. R. W. Peelle
44. S. Raman
45. RSIC
46. R. T. Santoro
47. P. H. Stelson
48. H. A. Todd
49. J. H. Todd
50. G. E. Whitesides
51. A. Zucker
52. P. Greebler (Consultant)
53. W. B. Loewenstein (Consultant)
54. R. E. Uhrig (Consultant)
55. R. Wilson (Consultant)
56-57. Central Research Library
58. ORNL Y-12 Technical Library
Document Reference Section
59-60. Laboratory Records Department
61. Laboratory Records ORNL RC
62. ORNL Patent Office

External Distribution

63. Office of Assistant Manager, Energy Research and Development, DOE-ORO, Oak Ridge, TN 37830
64. E. T. Ritter, Office of Basic Energy Sciences, Department of Energy, Washington, D.C. 20545
65. G. L. Rogosa, Office of Basic Energy Sciences, Division of Nuclear Science, Department of Energy, Washington, D.C. 20545
66. S. L. Whetstone, Office of Basic Energy Sciences, Department of Energy, Washington, D.C. 20545
67. P. B. Hemmig, Physics Branch, Division of Reactor Research and Technology, Department of Energy, Washington, D.C. 20545
68-69. C. D. Bowman and J. E. Lease, National Bureau of Standards, Center for Radiation Research, Nuclear Radiation Division, Washington, D.C. 20234
70. M. S. Moore, Los Alamos Scientific Laboratory, P.O. Box 1663, Los Alamos, NM 87544
71. R. C. Block, Rensselaer Polytechnic Institute, Troy, NY 12181
72. N. C. Pering, 611 Hansen Way, Palo Alto, CA 94303
73-99. Technical Information Center (TIC)